Large Scale Automatic Crater Rim Detection at the Lunar South Pole.

Ara V Nefian[1], Mark Shirley[2],Tony Colaprete[2], and Rick Elphic[2], [1]KBR, NASA Ames Research Center, MS 245-3, Moffett Field, CA, USA (ara.nefian@nasa.gov),[2]NASA

While manual crater detection is impractical given the large amount of data made available by lunar orbital missions, the accuracy of the automatic methods is often limited by the crater size, and by varying illumination conditions. The proposed fully automatic method has been tested successfully in large scale (24 km^2) image mosaics and digital elevation models (DEM) at the lunar Pole for craters down to 4m in diameter and captured in various illumination conditions. The results of this work have the potential to pave the way to the automated crater detection and characterization (including and age and size estimation) of the lunar surface with significant implications in science and mission operations.

Proposed Method

Automatic crater detection methods [1], [2], [3], [4], use as input either images or digital elevation models (DEM). The proposed method advances the crater detection method introduced in [5] by scaling the results to process areas up to 24 km^2, refining the crater rim detection, and increasing the ability to detect smaller craters down to 4pixel in size. The method uses a neural network classifier trained from manually labeled data . The labeled data consists of three classes: craters, flat regions with no craters and shadows. Craters are detected

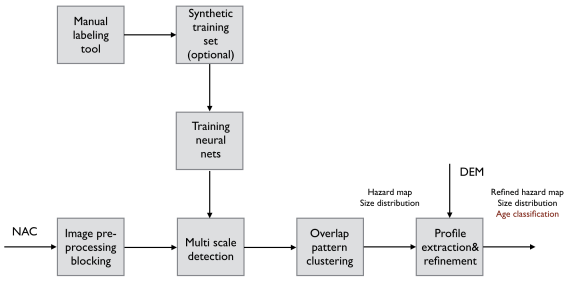

Figure 1: Overall crater detection system.

in each Lunar Reconaissaince Orbiter - Narrow Angle Camera (LRO-NAC) image separately. For each LRO-NAC image a new training set is built from the available labeled data using the illumination conditions (sun and spacecraft position) at which the LRO-NAC image was captured. This step avoids manual labeling for each image and plays a critical role in building a fully automated crater detection pipeline. The resulting detections from multiple images are combined to cover a specific DEM and image mosaic region(Figure 1). Finally, the crater position is refined to match the crater rims using the 3D elevation data. Figure 2 illustrates the crater detection result before and after the alignment with the DEM. The top row represents the crater profiles extracted along the main and secondary diagonal profiles of the square region where the craters are detected. The second row displays the same crater profiles after the local slope was removed. The dots on the the crater profiles indicate the location of the left rim, crater center (minimum elevation) and right crater respectively. These points on the crater profiles are used to refine the crater center and the radius. Finally, rows three and four display the circles associated with crater rims in the hillshaded DEM and image mosaic respectively. Note that our proposed method uses a cost function optimization method to improve the crater localization. The proposed cost function minimizes the errors between the coordinates of the crater rims and and crater center in the extracted crater profiles. The left and right columns in Figure 2 depict the crater profiles and location before and after alignment respectively.

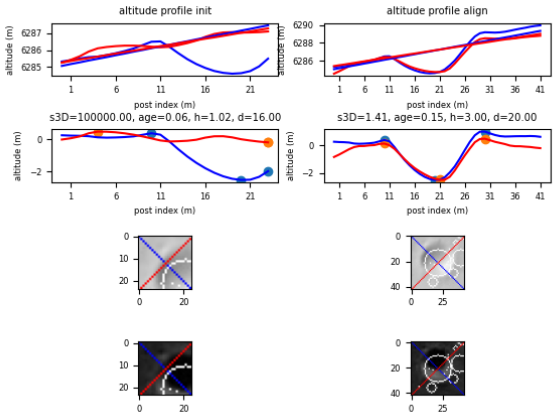

Figure 2: Elevation profiles, image and hillshade before (left) and after (right) alignment with the DEM.

Experimental Results

Figure 3 illustrates an area of 24km^2 at the lunar South Pole and the regions highlighted in white represents areas covered by the LRO-NAC imagery with sufficient illumination where the crater detection method was used. Fig-

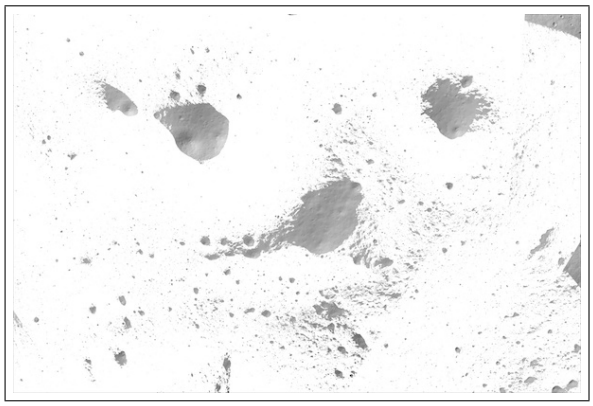

Figure 3: Area of the DEM (6km×4km) processed automatically is shown in white over the hillshaded DEM.

ure 4 illustrates the crater detection results over the entire hillshaded DEM processed. Figures 5 and 6 illustrate the

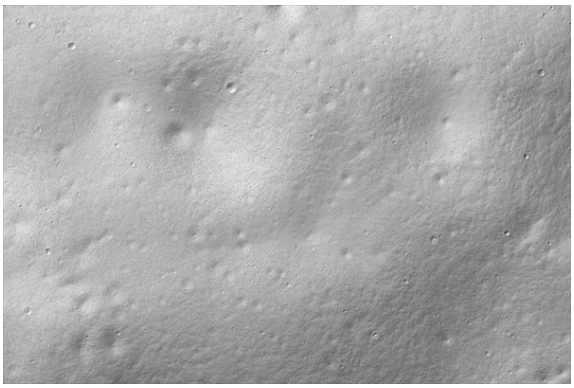

Figure 4: Hillshaded DEM of the lunar south pole area of interest.

crater detection results in subregions of the maximum lit mosaic and hillshaded DEM respectively.

Conclusions and Future Work

The work presented in this paper describes a fully automated, large scale method for precise crater detection down to four pixels in size. The technique uses the elevation model to precisely determine the crater rims and crater center. This method will be used to determine the crater depth to diameter ratios and provide an insight in the crater age at the lunar South Pole. The potential of the presented method to detect craters of various sizes in other lunar regions including the North pole and Equatorial regions will be further investigated.

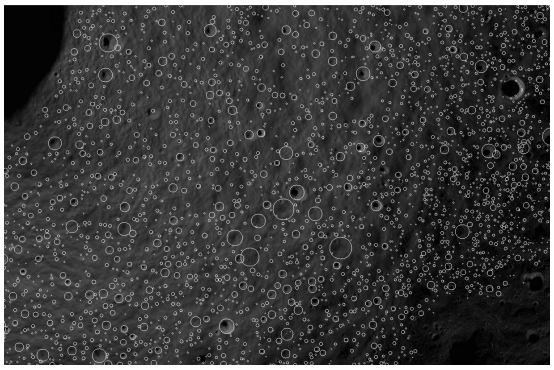

Figure 5: Crater detection results over a subregion of the maximum lit mosaic.

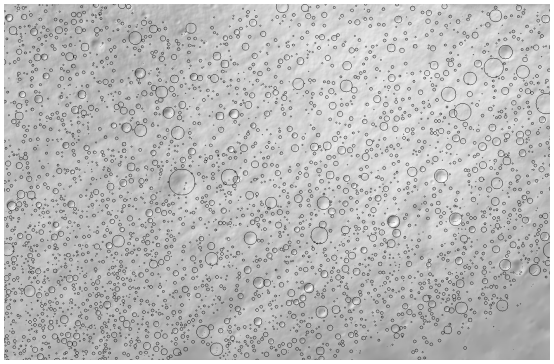

Figure 6: Crater detection results over a subregion of the hillshaded mosaic.

References

[1] J. P. Cohen, H. Z. Lo, T. Lu, and W. Ding. Crater detection via convolutional neural networks. *arXiv preprint arXiv:1601.00978.*, 2016.

[2] E. Emami, Bebis, G., A. Nefian, and T Fong. Automatic crater detection using convex grouping and convolutional neural networks. *International Symposium on Visual Computing*, 2015.

[3] S. Ren and et al. Faster r-cnn: Towards real- time object detection with region proposal networks. *Advances in neural information processing systems*, 2015.

[4] E. Emami, Bebis G., A. Nefian, and T. Fong. On crater verification using mislocalized crater regions. *IEEE Winter Conference on Applications of Computer Vision*, 2017.

[5] Ara V. Nefian, Mark Shirley, Tony Colaprete, and Rick Elphic. Automatic crater detection at the lunar south pole. *Lunar and Planet. Sci. Conf.*, 2021.